ID-663

Gaussian processes for slice-based super-resolution MR images

Hernán Darío Vargas Cardona[1], Andrés F. López-Lopera[1], Álvaro A. Orozco[1], Mauricio A. Álvarez[1], Juan Antonio Hernández Tamames[2] and Norberto Malpica[2]

[1]Faculty of Engineering, Universidad Tecnológica de Pereira, Pereira, Colombia.
[2]Laboratorio de análisis de imagen médica y Biometría, Universidad Rey Juan Carlos, Móstoles, Spain.

ISVC 2015: 11th International Symposium on Visual Computing
Las Vegas, Nevada, USA. December 14-16

Universidad Tecnológica de Pereira

Introduction

- Magnetic resonance imaging (MRI) is a medical technique used in radiology to obtain anatomical images. Due to hardware limitations and clinical protocols, MRI data are often acquired with low-resolution [1].
- The scientific community has been developing super-resolution (SR) methodologies in order to enhance spatial resolution.
- The enhancement of spatial resolution in MR images improves clinical procedures such as tissue segmentation, registration and disease diagnosis [2].
- Several methods to perform SR-MR images have been proposed. However, they present different drawbacks: sensitivity to noise, high computational cost, and complex optimization algorithms [3, 4].
- In this paper, we develop a supervised learning methodology to perform SR-MR images using a patch-based Gaussian process regression (GPR) method.

Materials and Methods

Super-resolution Gaussian process regression (SR-GPR)

A GP is completely defined by its mean function, $m(\mathbf{x})$, and covariance function, $k(\mathbf{x}, \mathbf{x}')$, such that [5]

$$f(\mathbf{x}) \sim \mathcal{GP}\left(m(\mathbf{x}), k(\mathbf{x}, \mathbf{x}')\right),$$

where $f(\mathbf{x})$ is the intensity value of pixel $\mathbf{x}$. Be a noisy image with a set of pixels and intensities $\{(\mathbf{x}_i, y_i)\}_{i=1}^n$, where its intensities follow the standard linear regression model $y_i = f_i + \varepsilon$, with $f_i = f(\mathbf{x}_i)$ and Gaussian noise $\varepsilon \sim \mathcal{N}(0, \sigma_n^2)$. The conditional distribution for test points is given by [5]

$$\mathbf{y}_*|\mathbf{X}, \mathbf{y}, \mathbf{X}_* \sim \mathcal{N}\left(\bar{\mathbf{y}}_*, \text{cov}(\mathbf{y}_*)\right),$$

with

$$\bar{\mathbf{y}}_* = \mathbf{K}_{\mathbf{y},\mathbf{y}_*}^\top [\mathbf{K}_{\mathbf{y},\mathbf{y}} + \sigma_n^2 \mathbf{I}]^{-1} \mathbf{y},$$

$$\text{cov}(\mathbf{y}_*) = \mathbf{K}_{\mathbf{y}_*,\mathbf{y}_*} + \sigma_n^2 \mathbf{I}_* - \mathbf{K}_{\mathbf{y},\mathbf{y}_*}^\top [\mathbf{K}_{\mathbf{y},\mathbf{y}} + \sigma_n^2 \mathbf{I}]^{-1} \mathbf{K}_{\mathbf{y},\mathbf{y}_*}.$$

Figure 1 shows the graphical model for a GPR adapted for single SR images using a 3×3 patch proposed in [6]. intensity of the target pixel we want to predict.

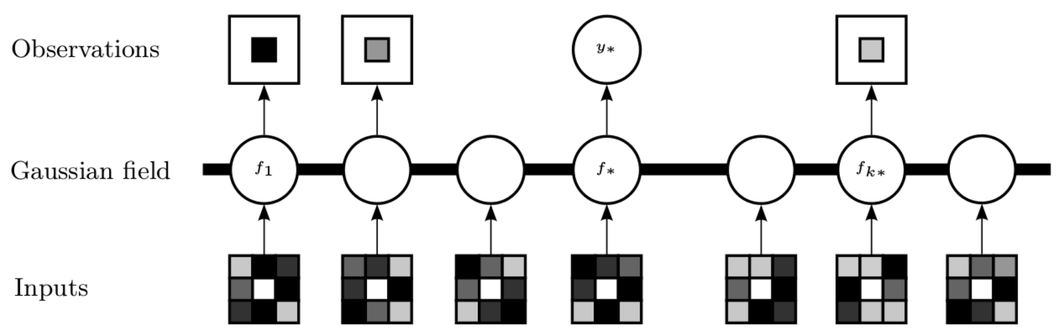

Figure: Graphical model for a GPR applied to a single super-resolution image using a 3×3 patch proposed in [6]. Squares represent observed pixels and circles represent unknown Gaussian fields. The inputs are the intensities of neighbor pixels (predictors), and the output are the intensity of target pixels we want to predict.

Experimental Background

Dataset: Images of the head were acquired on a General Electric Signa HDxt 3.0T MR scanner using the body coil for excitation, and an 8-channel quadrature brain coil for reception. Subjects were positioned supine with the arms down. The head was positioned in the head-neck coil (MRI). Imaging was performed using an isotropic 3D T1-weighted and 3D T2-weighted Spoiled Gradient Recalled (SPGR) sequence with a repetition time of 10.024 *ms*, an echo time of 4.56 *ms*, an inversion time of 600 *ms*, 1 number of excitations (NEX), an acquisition matrix of 512×512, a resolution of $1 \times 1 \times 1$ mm^3 per voxel, and a flip angle=12. The MRI-T1 and MRI-T2 studies are composed by 160 and 45 slices, respectively. The acquisition was performed using a parallel imaging factor of 2.

SR-GPR:

Algorithm 1 patch-based SR-GPR approach with filtering.

Require: LR (low-resolution image)
1: GPR-patch training: Maximum likelihood.
2: GPR-patch pixel inference: HR $\leftarrow \mathbf{y}_*|\mathbf{x}, \mathbf{y}, \mathbf{x}_* \sim \mathcal{N}\left(\bar{\mathbf{y}}_*, \text{cov}(\mathbf{y}_*)\right)$
3: 2D filtering stage: SR $\leftarrow$ HR $\otimes H$, with $H = [0\ {-1}\ 0\ ;\ {-1}\ 5\ {-1}\ ;\ 0\ {-1}\ 0]$
4: **return** SR (super-resolution image)

Figure: patch-based SR-GPR approach with filtering.

Results and Discussion

Super-resolution MR images validation

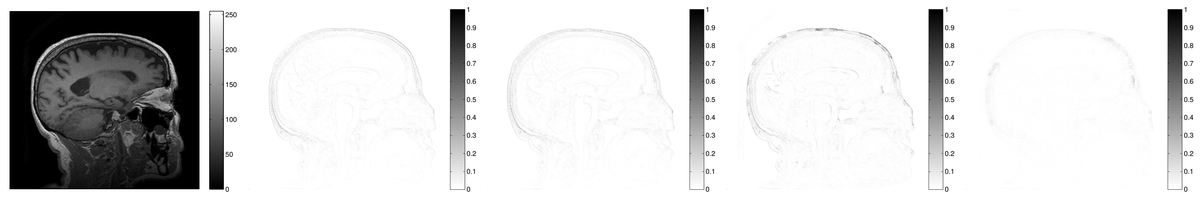

(a) (b) B-spline (c) nearest-neighbor (d) SR-GPR1 (e) SR-GPR2

Figure: Ground truth and graphic errors for super-resolution (SR) MRI images validation. The ground truth for T1 slice-100 is showed in (a).

Table: Average MSE results obtained for T1 and T2 respect to the MRI ground truth

	B-spline	NN	SR-GPR1	SR-GPR2
MR study	$\mu \pm \sigma$	$\mu \pm \sigma$	$\mu \pm \sigma$	$\mu \pm \sigma$
T1	27.95 ± 7.282	38.12 ± 10.45	55.89 ± 20.47	$\mathbf{7.806 \pm 1.552}$
T2	48.83 ± 13.14	60.44 ± 16.05	72.99 ± 22.12	$\mathbf{25.65 \pm 7.659}$

Morphological validation

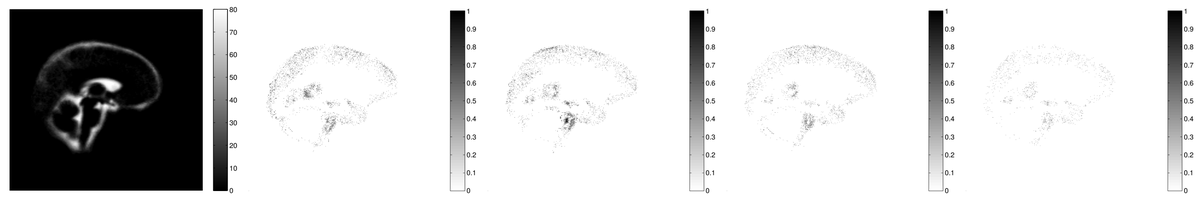

(a) (b) B-spline (c) nearest-neighbor (d) SR-GPR1 (e) SR-GPR2

Figure: Ground truth and graphic errors for morphological validation. Using the T1 slice-100 from Figure 3, the gold standard of CSF is showed in (a)

Table: Average MSE results obtained respect to the gold standard tissue segmentations.

	B-splines	NN	SR-GPR1	SR-GPR2
Tissue	$\mu \pm \sigma$	$\mu \pm \sigma$	$\mu \pm \sigma$	$\mu \pm \sigma$
CSF	0.0154 ± 0.0142	0.0148 ± 0.0140	0.0079 ± 0.0064	$\mathbf{0.0044 \pm 0.0040}$
WM	0.0362 ± 0.0297	0.0357 ± 0.0322	0.0166 ± 0.0124	$\mathbf{0.0084 \pm 0.0065}$
GM	0.0422 ± 0.0300	0.0406 ± 0.0312	0.0203 ± 0.0132	$\mathbf{0.0105 \pm 0.0071}$

Conclusion

- In this paper we presented a methodology for super-resolution magnetic resonance (SR-MR) images based on supervised learning.
- We modeled a Gaussian process regression for 2D multi-slice SR images (SR-GPR2). In order to enhance edge regions, we applied a 2D filtering stage.
- Results achieved with our proposal outperform to B-spline interpolation, nearest-neighbor, and the GPR method developed in [6].
- Our methodology performs better in both SR reconstruction images and morphological validation, making SR-GPR2 a promising approach to enhance spatial resolution in brain MR images.

Acknowledgment

H.D. Vargas Cardona is funded by Colciencias under the program: *formación de alto nivel para la ciencia, la tecnología y la innovación - Convocatoria 617 de 2013*. This research has been developed under the project: *Estimación de los parámetros de neuro modulación con terapia de estimulación cerebral profunda en pacientes con enfermedad de Parkinson a partir del volumen de tejido activo planeado*, financed by Colciencias with code 1110-657-40687.

References

J. Isaac and J. Kulkarni, "Super resolution techniques for medical image processing," in *International Conference on Technologies for Sustainable Development (ICTSD)*, 2015, pp. 1–6.

K. Malczewski, "Inter-K-space motion based strategy for super-resolution in MRI," in *17th European Signal Processing Conference*, 2009, pp. 30–34.

A. Rueda, N. Malpica, and E. Romero, "Single-image super-resolution of brain MR images using overcomplete dictionaries," *Medical Image Analysis*, vol. 17, no. 1, pp. 113–132, 2012.

Y. Wang, J. Qiao, L. Jun-bao, A. Ping-Fu, C. Shu-Chuan, and J. Rodd, "Sparse representation-based MRI super-resolution reconstruction," *Measurement*, vol. 47, pp. 946–953, 2012.

C. E. Rasmussen and C. K. I. Williams, *Gaussian Processes for Machine Learning (Adaptive Computation and Machine Learning)*. The MIT Press, 2005.

H. He and W.-C. Siu, "Single image super-resolution using Gaussian process regression," in *IEEE Conference on Computer Vision and Pattern Recognition (CVPR)*, June 2011, pp. 449–456.

{hernan.vargas,anfelopera,malvarez,aaog}@utp.edu.co, {norberto.malpica,juan.tamames}@urjc.es